

1 **Published in Nature: 21st Feb 2013, vol 494, p349-353**

2
3 **Ecosystem resilience despite large-scale altered hydroclimatic condition**

4 **Guillermo E. Ponce Campos^{1,2}, M. Susan Moran¹, Alfredo Huete³, Yongguang Zhang¹,**
5 **Cynthia Bresloff², Travis E. Huxman⁴, Derek Eamus³, David D. Bosch⁵, Anthony R.**
6 **Buda⁶, Stacey A. Gunter⁷, Tamara Heartsill Scalley⁸, Stanley G. Kitchen⁹, Mitchel P.**
7 **McClaran¹⁰, W. Henry McNab¹¹, Diane S. Montoya¹², Jack A. Morgan¹³, Debra P.C.**
8 **Peters¹⁴, E. John Sadler¹⁵, Mark S. Seyfried¹⁶, Patrick J. Starks¹⁷**

9 ¹*USDA ARS Southwest Watershed Research, Tucson, Arizona 85719, USA*

10 ²*Soil, Water & Environmental Sciences, University of Arizona, Tucson, Arizona 85721, USA*

11 ³*Plant Functional Biology and Climate Change Cluster, University of Technology Sydney, NSW 2007, Australia*

12 ⁴*Ecology & Evolutionary Biology, University of California, Irvine, California, USA and Center for Environmental*
13 *Biology, University of California, Irvine, California, 92697, USA*

14 ⁵*USDA ARS Southeast Watershed Research Laboratory, Tifton, Georgia 31793, USA*

15 ⁶*USDA ARS Pasture Systems & Watershed Management Research Unit, University Park, Pennsylvania 16802, USA*

16 ⁷*USDA ARS Southern Plains Range Research Station, Woodward, Oklahoma 73801, USA*

17 ⁸*USDA FS International Institute of Tropical Forestry, Rio Piedras, 00929, Puerto Rico*

18 ⁹*USDA FS Rocky Mountain Research Station Shrub Sciences Laboratory, Provo, Utah 84606, USA*

19 ¹⁰*School of Natural Resources and the Environment, University of Arizona, Tucson, Arizona 85721, USA*

20 ¹¹*USDA FS NC, Asheville, North Carolina 28806, USA*

21 ¹²*USDA FS Pacific Southwest Research Station, Arcata, California 95521, USA*

22 ¹³*USDA ARS Rangeland Research Laboratory, Fort Collins, CO 80526, USA*

23 ¹⁴*USDA ARS Jornada Experimental Range and Jornada Basin Long Term Ecological Research Program, New*
24 *Mexico State University, Las Cruces, New Mexico 88012, USA*

25 ¹⁵*USDA ARS Cropping Systems & Water Quality Research Unit, Columbia, Missouri 65211, USA*

26 ¹⁶*USDA ARS Northwest Watershed Research Center, Boise, Idaho 83712, USA*

27 ¹⁷*USDA ARS Grazinglands Research Laboratory, El Reno, Oklahoma 73036, USA*

28
29 **Climate change is predicted to increase both drought frequency and duration, and when**
30 **coupled with substantial warming, will establish a new hydroclimatologic paradigm for**
31 **many regions¹. Large-scale, warm droughts have recently occurred in North America,**
32 **Africa, Europe, Amazonia, and Australia, resulting in major impacts on terrestrial**
33 **ecosystems, carbon balance, and food security^{2,3}. Here we compare the functional response**
34 **of above-ground net primary production (ANPP) to contrasting hydroclimatic periods in**
35 **the late-20th-century (1975-1998) and drier, warmer conditions in the early 21st century**
36 **(2000-2009) in the Northern and Southern Hemispheres. We found a common ecosystem**
37 **water-use efficiency (WUE_e: ANPP/evapotranspiration) across biomes ranging from**
38 **grassland to forest that indicates an intrinsic system sensitivity to water availability across**
39 **rainfall regimes, regardless of hydroclimatic conditions. We found higher WUE_e in drier**
40 **years that increased significantly with drought to a maximum WUE_e (WUE_x) across all**
41 **biomes; and a minimum native state (WUE_n) that was common across hydroclimatic**
42 **periods. This indicates biome-scale resilience to the inter-annual variability associated with**
43 **the early 21st century drought – e.g., the capacity to tolerate low annual precipitation and**
44 **to respond to subsequent periods of favorable water balance. These findings provide a**
45 **conceptual model of ecosystem properties at the decadal scale applicable to the wide-spread**
46 **altered hydroclimatic conditions that are predicted for later this century. Understanding**

47 **the hydroclimatic threshold that will break down ecosystem resilience and alter WUE_x may**
48 **allow us to predict landsurface consequences as large regions become more arid, starting**
49 **with water-limited, low-productivity grasslands.**

50 Increased aridity and persistent droughts are projected in the 21st century for most of Africa,
51 southern Europe and the Middle East, most of the Americas, Australia, and Southeast Asia¹.
52 This is predicted to dramatically change vegetation productivity across ecosystems from
53 grasslands to forests^{2,4,5} with direct impact on societal needs for food security and basic
54 livelihood⁶. However, model predictions of productivity responses can only provide most-likely
55 scenarios of the impact of climate change, and few experiments have focused on how anticipated
56 changes in precipitation might be generalized across terrestrial ecosystems⁹. Long-term
57 measurements of natural variability in field settings, supported by manipulative experiments, are
58 considered the best approach for determining the impact of prolonged drought on vegetation
59 productivity^{6,7}.

60 In field experiments, vegetation productivity is generally measured as the above-ground net
61 primary production (ANPP, or total new organic matter produced above-ground during a specific
62 interval⁸) and vegetation response to changes in precipitation is quantified as rain-use efficiency
63 (RUE), defined as the ratio of ANPP to precipitation over a defined season or year⁹. Using this
64 approach, continental-scale patterns of RUE have been reported for extended periods in the late
65 20th century¹⁰. Ecosystem water-use efficiency (WUE_e : ANPP/evapotranspiration¹¹) provides
66 additional insight into the ecological functioning of the land surface, where evapotranspiration
67 (ET) is calculated as precipitation minus the water lost to surface runoff, recharge to
68 groundwater and changes to soil water storage¹² (Supplementary Appendix II). Here we
69 compare the functional responses of RUE and WUE_e to local changes in precipitation to
70 document ecosystem resilience – the capacity to absorb disturbances and retain the same
71 function, feedbacks, and sensitivity¹³ – during altered hydroclimatic conditions¹⁴.

72 The objective was to determine how ANPP across biomes responded to altered hydroclimatic
73 conditions forced by the contemporary drought in the Southern and Northern Hemispheres. This
74 study is based on measurements made during the period from 2000-2009 at 12 United States
75 Department of Agriculture (USDA) long-term experimental sites in the conterminous United
76 States and Puerto Rico, and 17 similar sites in the Australian continent over a range of
77 precipitation regimes (termed USDA₀₀₋₀₉ and Australia₀₁₋₀₉, respectively). To contrast
78 productivity under altered hydroclimatic conditions with precipitation variability in the late 20th
79 century, we compared results from the 2000-2009 period with similar analysis of measurements
80 made during the period from 1975-1998¹⁰. The latter measurements were made primarily at
81 Long-term Ecological Research (LTER) locations, with 14 sites – 12 in North America and 2 in
82 Central and South America - hereafter referred to as the LTER₇₅₋₉₈ dataset. For a subset of the
83 LTER₇₅₋₉₈ sites, ANPP measurements were continued during the period from 2000-2009 (termed
84 LTER₀₀₋₀₉) and these were used for further validation of the results (Supplementary Table A1).

85 The warm drought during the early 21st century in the US, Europe and Australia has been
86 recognized as a significant change from the climatological variability of the late 20th century^{1,15}.
87 Globally, the 2000-2009 decade ranked as the 10 warmest years of the 130-year (1880-2009)
88 record¹⁶. Global annual evapotranspiration increased on average by 7.1 mm/yr/decade from
89 1982-1997, and after that, remained at a plateau through 2008¹⁷, thereby revealing the impact of
90 the drought on this important Earth surface process¹⁷. In the United States, heat waves in 2005,

91 2006 and 2007 broke all-time records for high maximum and minimum temperatures, and drier
92 than average conditions were reported for over 50% of the conterminous US in 2000-2002 and
93 2006-2007¹⁸. In Australia, the widespread 6-year drought from 2001 to 2007 was recorded as
94 the most severe in the nation's history¹⁹. The mean Palmer Drought Severity Index²⁰ (PDSI;
95 Supplementary Appendix II) for USDA and Australian sites decreased significantly ($P < 0.002$)
96 from 1980-1999 to 2000-2009 (USDA) and 2001-2009 (Australia), declining from -0.06 to -0.81
97 and from 0.09 to -1.34, respectively, where a reduction in the PDSI indicates an increase in
98 aridity. Furthermore, warm-season temperatures at USDA and Australian sites during the 2000-
99 2009 and 2001-2009 periods, respectively, were significantly higher ($P < 0.014$) than 1980-1999
100 averages, warming by 0.32 and 0.44 °C, respectively.

101 The Enhanced Vegetation Index (EVI²¹) satellite observations from the Moderate Resolution
102 Imaging Spectroradiometer (MODIS) were integrated annually (termed iEVI) as an empirical
103 proxy for ANPP at USDA₀₀₋₀₉ and Australia₀₁₋₀₉ sites (Supplementary Appendix II). There are
104 multiple publications suggesting that this is a robust approximation of collective plant behavior²³,
105 and here, we quantified the accuracy of this relation for the biomes, years and precipitation
106 patterns of this study. *In situ* estimates of ANPP made with conventional field assessment
107 methods (ANPP_G) during the period 2000-2009 were compiled for 10 sites across the United
108 States (Supplementary Table A2) and compared with iEVI measurements for the same site and
109 year (Figure 1). A log-log regression resulted in an equation that was used to estimate ANPP
110 from iEVI values (ANPP_S), where $ANPP_S = 51.42 \times iEVI^{1.15}$ resulting in a strong correlation
111 between ANPP_G and ANPP_S for this dataset (Figure 1).

112

113 **Cross-biome WUE_e during altered hydroclimatic condition**

114 The response of plant production to precipitation during the contemporary hydroclimatic
115 conditions of prolonged warm drought showed strong agreement with the ANPP/precipitation
116 relations reported during the late 20th century¹⁰ (Figure 2a). The lowest mean RUE (i.e., slope of
117 the ANPP/precipitation relation) reported for biomes with the highest mean precipitation can be
118 explained largely (though not completely¹⁰) by the rain water that is not available for plant
119 production due to runoff, groundwater recharge and increased soil water storage. Thus, the
120 increase in water available for vegetation production with increasing precipitation is partially
121 consumed by non-biological components of the hydrologic cycle (i.e., runoff and deep drainage).
122 This is particularly true during entrenched drought due to additional storage-refill capacity²⁴ of a
123 soil profile that has been depleted of water during prolonged drought. This becomes apparent
124 when production was plotted as a function of evapotranspiration: the mean ecosystem water-use
125 efficiency (WUE_m) was constant across the entire precipitation gradient (Figure 2b). Further,
126 there were no significant differences among WUE_m between the three datasets ($P > 0.05$ per
127 homogeneity of regression slope test²⁵). Combined, this indicated that all biomes retained their
128 intrinsic sensitivity to water availability during prolonged, warm drought conditions. This fact
129 suggests that the rules governing how species are organized in terms of their tolerance of
130 hydrological stress are robust despite extended perturbation by low precipitation²⁶.

131 When water limitations at each site were most severe (for the driest years in each multi-year
132 record), a maximum ecosystem WUE (WUE_x) across all biomes was revealed for each of the 3
133 datasets (Figure 3a). The WUE_x was significantly higher for the Australia₀₁₋₀₉ sites (PDSI=-

134 1.34) than for the LTER₇₅₋₉₈ and USDA₀₀₋₀₉ sites (PDSI₋₀ and PDSI_{-0.81}, respectively) ($P <$
135 0.05^{25} , Figure 3a inset). This implies a cross-biome sensitivity to prolonged warm drought
136 where ecosystems sustain productivity in the driest years by increasing their WUE_e. It also
137 indicates that in the driest year of the recent prolonged warm drought, water limitations
138 overshadowed the limitations imposed by other resources even at high-productivity sites. The
139 increase in cross-biome WUE_x with declining PDSI suggests that most biomes were primarily
140 water limited during the driest years of the early 21st century drought.

141 As a test of ecosystem resilience, a similar comparison was made for the wettest years during
142 mid- to late-drought (2003-2009) and compared to the results for the wettest years during the
143 earlier hydroclimatic conditions from 1975-1998. For the wettest years in both periods, we
144 found a minimum value (WUE_n) that was common to all biomes and similar across both
145 hydroclimatic periods (Figure 3b). The finding that WUE_n did not vary ($P > 0.05^{25}$) across
146 different hydroclimatic periods indicates a cross-biome capacity to respond to high annual
147 precipitation, even during periods of warm drought. The decrease from maximum to minimum
148 WUE_e ranged from 14% (for the USDA₀₀₋₀₉ and LTER₇₅₋₉₈ datasets) to 35% (for the Australia₀₁₋
149 ₀₉ dataset) and is hypothesized to occur through additional resource constraints that come into
150 play in wet years, including light and nutrient limitations^{10,26}. However, it may also be true that
151 mechanistic relationship between the two time-periods is not consistent, where shifts in
152 contemporary species composition as a result of drought influenced this landscape-scale process.

153 The ability of plants to increase WUE_x and retain historic WUE_n during altered hydroclimatic
154 conditions suggest that the factors controlling these two processes are different with respect to
155 how climate and the vegetation assemblage are changing. During the driest years, there was a
156 cross-biome adjustment in WUE_e that increased with drought intensity, thus sustaining
157 production at near late-20th-century levels during prolonged drought. In the wettest years, the
158 sites exhibited an ability to absorb the disturbances associated with the early 21st century drought
159 and retained the same sensitivity of ANPP to water availability across both hydroclimatic
160 periods. These different responses to precipitation extremes may be due to changes in vegetation
161 structure and function, and plant-soil feedbacks that are not captured in the integrated analysis of
162 either RUE or WUE_e. These must be considered in a full assessment of ecosystem vulnerability
163 or resistance to change.

164

165 **Ecosystem resilience during altered hydroclimatic condition**

166 In this study, ecosystem resilience was measured as the capacity of ecosystems to absorb
167 disturbances associated with the early 21st century drought and retain late-20th-century sensitivity
168 of ANPP to high annual water availability. Our analyses suggest an intrinsic sensitivity of plant
169 communities to water availability, and a shared capacity to tolerate low annual precipitation but
170 also to respond to high annual precipitation. These findings provide a conceptual model of
171 ecosystem resilience at the decadal scale during the altered hydroclimatic conditions that are
172 predicted for later this century¹ (Figure 4). During the driest years, the high-productivity sites
173 became water limited to a greater extent resulting in higher WUE_e similar to that encountered in
174 less productive, more arid ecosystems. It follows that when all ecosystems are primarily water
175 limited, a cross-biome maximum WUE_e will be reached (WUE_x), and that this cross-biome likely
176 has a maximum value cannot be sustained with further reductions in water availability. Further,

177 we predict that as cross-biome WUE_e reaches that maximum WUE_x value, WUE_n will approach
178 WUE_x because production will be limited largely by water supply and less so by nutrients and
179 light (Figure 4).

180 With continuing warm drought, the single linear ANPP/ET relation that forms the common
181 cross-biome WUE_e would collapse as biomes endure the significant drought-induced mortality
182 that has been extensively documented over the past decade^{2,5}. This loss of resilience associated
183 with dieback would likely occur first for ecosystems that respond most rapidly to precipitation
184 variability (i.e., grasslands^{27,28}). Thus, the cross-biome ANPP/ET relation would become non-
185 linear as WUE_x and WUE_n approached zero for the most water-limited, low-productivity sites,
186 while WUE_e values would be less impacted in the high-productivity sites. Subsets of the
187 LTER₇₅₋₉₈ (n=4), USDA₀₀₋₀₉ (n=5) and Australia₀₁₋₀₉ (n=2) datasets limited to grassland sites
188 across a semiarid-to-mesic precipitation gradient were used to corroborate this prediction (Figure
189 4 inset). During this study period, grassland WUE_x decreased with increasing aridity (decreasing
190 PDSI) indicating an increasing lack of resilience with prolonged warm drought in these biomes,
191 as predicted. This implies that these systems are closer to a threshold which, when crossed, will
192 result in biome reorganization.

193

194 **Discussion**

195 Here we quantified the impact of the early 21st century drought on ecosystem productivity and
196 resilience across many sites on 2 continents. Cross-biome capacities and sensitivities of
197 production were maintained through prolonged warm drought by increases of WUE_e during the
198 driest years and a resilience during wet years indicated by a common WUE_e across both
199 hydroclimatic periods. The conclusions are particularly compelling because they are based on
200 measurements across multiple biomes with comparisons of multi-year periods of altered
201 hydroclimatic conditions. These findings were extended to predictions that, if warm drought
202 continues, significant mortality, particularly in low-productivity grasslands that are most
203 sensitive to water availability may threaten ecosystem resilience across biomes given the
204 substantial changes in ecosystem structure. The emergence of these patterns at the spatial and
205 temporal scale at which they were derived requires investigation of the supporting
206 ecohydrological mechanisms that underlie the complex plant-soil couplings. Spatially, this work
207 represents broad cross-biome behavior but does not fully represent the complex site-level
208 response to prolonged warm drought. The site-level mechanisms associated with disease, pests,
209 fire, response lags, species replacement and meristem density in forests² and grasslands^{4,27,29}
210 complicate specific processes maintaining or impacting cross-biome resilience of ecosystem
211 function. Further, there are predictions of a general biogeochemical resetting as increases in
212 carbon dioxide supply affect a multitude of plant and soil processes³⁰. Temporally, these
213 predictions of ecosystem resilience were based on behavior at the scale of a decade or longer,
214 including a period of prolonged warm drought. With careful application of this satellite-based
215 metric, it is possible to continue monitoring cross-biome ecosystem resilience at selected cross-
216 continental sites year-by-year into the future as we develop a greater understanding of the
217 physical and biological mechanisms controlling these patterns.

218 **Methods Summary**

219 Daily precipitation and temperature were measured at *in-situ* stations and represented a
220 homogeneous vegetated area of ~2x2 km and no major disturbances (e.g. fires) during the 2000-
221 2009 period. Total and mean annual precipitation were computed from daily values over the
222 study period during the hydrologic year (October – September for the U.S. and May-April for
223 Australia). PDSI values at each location were computed using the corresponding precipitation,
224 temperature and soil water holding capacity data. For the Enhanced Vegetation Index (EVI),
225 images (tiles) from the MODIS website were downloaded to extract a measurement every 16-
226 days at 250m spatial resolution for each site involved. Quality assurance (QA) at the pixel level
227 was applied before window sizes of 9x9 pixels were averaged, including only those pixels that
228 passed the QA control. The resulting time series were smoothed in order to extract more accurate
229 annual integrated EVI values. Estimates of mean annual evapotranspiration were obtained for
230 all the sites by incorporating annual precipitation and percentages of forested and herbaceous
231 cover in a model derived from over 250 catchment-scale measurements from around the world¹².
232

233 **References**

- 234 1. Dai, A. Drought under global warming: a review. *Wiley Interdisciplinary Reviews: Climate*
235 *Change* **2**, 45–65 (2011).
- 236 2. Breshears, D. D. *et al.* Regional vegetation die-off in response to global-change-type
237 drought. *Proc. Natl Acad. Sci. USA* **102**, 15144 –15148 (2005).
- 238 3. Saleska, S. R., Didan, K., Huete, A. R. & da Rocha, H. R. Amazon forests green-up during
239 2005 drought. *Science* **318**, 612 (2007).
- 240 4. Scott, R. L., Hamerlynck, E. P., Jenerette, G. D., Moran, M. S. & Barron-Gafford, G. A.
241 Carbon dioxide exchange in a semidesert grassland through drought-induced vegetation
242 change. *J. Geophys. Res.* **115**, 12 PP. (2010).
- 243 5. Allen, C. D. *et al.* A global overview of drought and heat-induced tree mortality reveals
244 emerging climate change risks for forests. *Forest Ecol Manag* **259**, 660–684 (2010).
- 245 6. Milly, P. C. D. *et al.* Stationarity is dead: Whither water management? *Science* **319**, 573 –
246 574 (2008).
- 247 7. Weltzin, J. F. *et al.* Assessing the response of terrestrial ecosystems to potential changes in
248 precipitation. *BioScience* **53**, 941–952 (2003).
- 249 8. Roxburgh, S. H., Berry, S. L., Buckley, T. N., Barnes, B. & Roderick, M. L. What is NPP?
250 Inconsistent accounting of respiratory fluxes in the definition of net primary production.
251 *Funct Ecol* **19**, 378–382 (2005).
- 252 9. Le Houérou, H. N. Rain use efficiency: a unifying concept in arid-land ecology. *J Arid*
253 *Environ* **7**, 213 (1984).
- 254 10. Huxman, T. E. *et al.* Convergence across biomes to a common rain-use efficiency. *Nature*
255 **429**, 651–654 (2004).
- 256 11. Monson, R. *et al.* Tree species effects on ecosystem water-use efficiency in a high-elevation,
257 subalpine forest. *Oecologia* **162**, 491–504 (2010).
- 258 12. Zhang, L., Dawes, W. R. & Walker, G. R. Response of mean annual evapotranspiration to
259 vegetation changes at catchment scale. *Water Resour. Res.* **37**, PP. 701–708 (2001).
- 260 13. Walker, B., Holling, C. S., Carpenter, S. R. & Kinzig, A. Resilience, adaptability and
261 transformability in social – ecological systems. *Ecol Soc* **9**, 5 (2004).
- 262 14. Holling, C. S. Resilience and stability of ecological systems. *Annu Rev Ecol Syst* **4**, 1–23
263 (1973).

- 264 15. MacDonald, G. M. Water, climate change, and sustainability in the southwest. *Proc. Natl*
265 *Acad. Sci. USA* **107**, 21256–21262 (2010).
- 266 16. NOAA US climate division data plots. at <<http://www.esrl.noaa.gov/psd/data/usclimdivs/>>
- 267 17. Jung, M. *et al.* Recent decline in the global land evapotranspiration trend due to limited
268 moisture supply. *Nature* **467**, 951–954 (2010).
- 269 18. NDMC U.S. Drought Monitor. (2012).at
270 <<http://drought.unl.edu/MonitoringTools/USDroughtMonitor.aspx>>
- 271 19. BOM, A. Australia’s high-quality climate change datasets, Bureau of Meteorology.
272 *Australia’s High-Quality climate change datasets* (2011).at
273 <<http://www.bom.gov.au/climate/change/datasets/datasets.shtml>>
- 274 20. Palmer, W. C. Meteorological drought. *Weather Bureau Res. Paper No.45* (1965).
- 275 21. Huete, A. *et al.* Overview of the radiometric and biophysical performance of the MODIS
276 vegetation indices. *Remote Sens Environ* **83**, 195–213 (2002).
- 277 22. Running, S. W. *et al.* A Continuous Satellite-Derived Measure of Global Terrestrial Primary
278 Production. *BioScience* **54**, 547 (2004).
- 279 23. Goward, S. N., Tucker, C. J. & Dye, D. G. North American vegetation patterns observed
280 with the NOAA-7 advanced very high resolution radiometer. *Vegetatio* **64**, 3–14 (1985).
- 281 24. Sayama, T., McDonnell, J. J., Dhakal, A. & Sullivan, K. How much water can a watershed
282 store? *Hydrol Process* **25**, 3899–3908 (2011).
- 283 25. Huitema, B. E. *The analysis of covariance and alternatives*. (Wiley: 1980).
- 284 26. Jenerette, G. D., Barron-Gafford, G. A., Guswa, A. J., McDonnell, J. J. & Villegas, J. C.
285 Organization of complexity in water limited ecohydrology. *Ecohydrology*
286 (2011).doi:10.1002/eco.217
- 287 27. Knapp, A. K. & Smith, M. D. Variation among biomes in temporal dynamics of
288 aboveground primary production. *Science* **291**, 481–484 (2001).
- 289 28. Baldocchi, D. Global change: The grass response. *Nature* **476**, 160–161 (2011).
- 290 29. Morgan, J. A. *et al.* C4 grasses prosper as carbon dioxide eliminates desiccation in warmed
291 semi-arid grassland. *Nature* **476**, 202–205 (2011).
- 292 30. Peters, D. P. C., Yao, J., Sala, O. E. & Anderson, J. P. Directional climate change and
293 potential reversal of desertification in arid and semiarid ecosystems. *Glob Change Biol* **18**,
294 151–163 (2012).

295
296
297 **Full methods** and any associated references are available in the online version of the paper at
298 www.nature.com/nature.

299 **Supplementary Information** is linked to the online version of the paper at
300 www.nature.com/nature.

301 **Acknowledgements** The work was supported in part by the NASA SMAP Science Definition
302 Team under agreement 08-SMAPSDT08-0042 and the Australian Research Council (ARC)
303 Discover Project [DP1115479].

304 **Author Contributions** GEPC, MSM and AH conceived the study, assembled the data, and
305 produced the preliminary results. The remaining authors collected and analyzed data, and
306 contributed to the interpretation of results. All authors contributed to writing the paper.
307 Statistical analyses were performed by GEPC.

308 **Author information** Reprints and permissions information is available at
309 www.nature.com/reprints. The authors declare no competing financial interests. Readers are
310 welcome to comment on the online version of this article at www.nature.com/nature.
311 Correspondence and requests for materials should be addressed to GEPC (geponce@gmail.com)
312 or MSM (susan.moran@ars.usda.gov).

313 **Figure Captions:**

314 **Figure 1. Relation between ANPP and iEVI.** Relation between annual *in situ* estimates of
315 vegetation production (ANPP_G) and the corresponding iEVI derived from MODIS data during
316 the 2000-2009 period for 10 selected sites across multiple biomes (Table A2). The solid line
317 represents the linear regression ($R^2=0.82$, $P<0.0001$) used to estimate ANPP from iEVI values
318 (ANPP_S), where $ANPP_S=51.42 \times iEVI^{1.15}$. The inset shows the correlation between estimates of
319 ANPP_S and ANPP_G for the 10 sites over multiple years with $R=0.94$ and root mean squared error
320 (RMSE)=79 g m⁻².

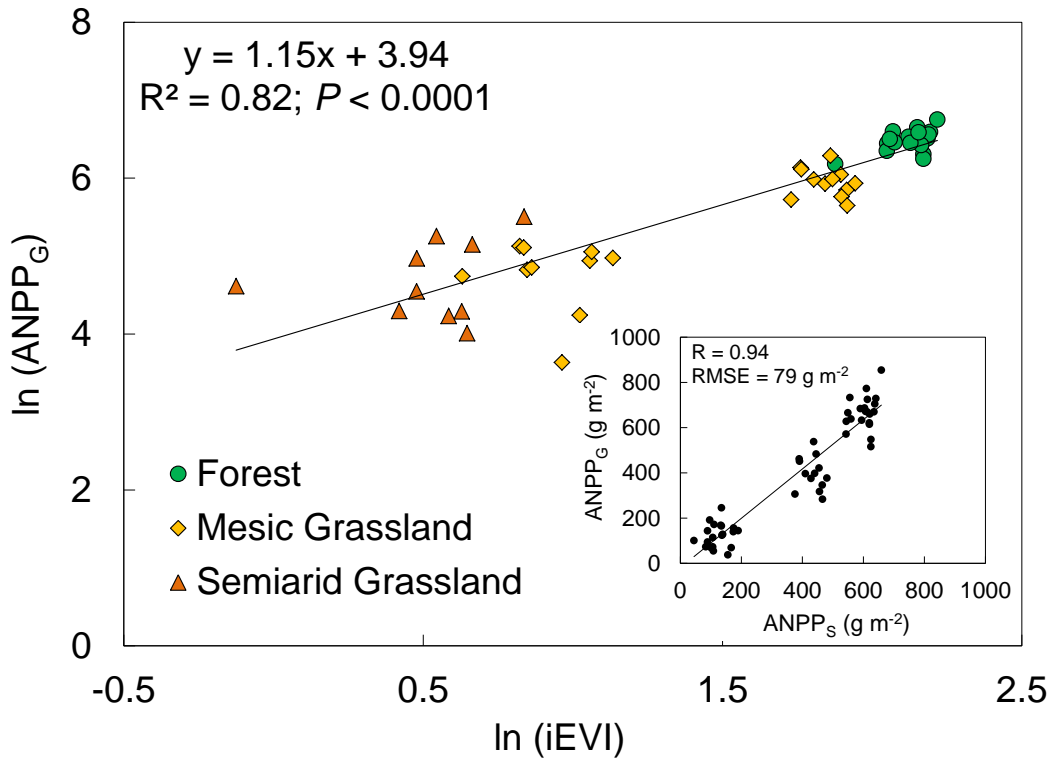
321 **Figure 2. Cross-biome sensitivity to precipitation during altered hydroclimatic condition.**
322 Relation of plant production to **a)** precipitation and **b)** evapotranspiration (ET) across
323 precipitation regimes during the late 20th century (LTER₇₅₋₉₈, green) and during altered
324 hydroclimatic conditions characterized by prolonged, warm drought (USDA₀₀₋₀₉ and Australia₀₁₋
325 ₀₉, red), showing significant coefficients of determination in best-fit regressions for each dataset
326 ($P<0.0001$). Symbols represent the mean values for each site over the multi-year study period.
327 Three LTER sites with *in situ* estimates of ANPP_G during the 2000-2009 period (black) were
328 included for qualitative validation of results with ANPP_S. The Figure 2b inset illustrates
329 differences in mean water-use efficiencies (WUE_m: the slope of the ANPP/ET relation) across
330 hydroclimatic conditions, where PDSI ranged from ~0 to -1.34 and columns labeled with the
331 same letter are not significantly different ($P > 0.05^{25}$).

332 **Figure 3. Ecosystem resilience across biomes and hydroclimatic conditions.** **a)** Maximum
333 (WUE_x) and **b)** minimum (WUE_n) water use efficiency, defined by the slope of the
334 ANPP/evapotranspiration relation in the driest years and wettest years, respectively, based on all
335 sites for each dataset, plus the three LTER₀₀₋₀₉ validation sites. The insets illustrate the
336 differences in **a)** WUE_x and **b)** WUE_n with mean PDSI for the study periods and locations, where
337 columns labeled with the same letter are not significantly different ($P > 0.05^{25}$) across
338 hydroclimatic conditions.

339 **Figure 4. A conceptual model of ecosystem resilience during altered hydroclimatic**
340 **condition.** **a)** A summary of WUE_e results in this study (solid lines), overlain with the predicted
341 behavior of WUE_x (brown dashed line) and WUE_n (blue dashed line) along a continuum of sites
342 limited primarily by water and by other resources with an arbitrary distinction made here at
343 $ET=700 \text{ mm yr}^{-1}$ for illustration only (black dashed line). Predictions are based on forecasts of
344 continuing warm drought, resulting in more high-productivity sites that are primarily water
345 limited and an increase in cross-biome maximum WUE_x. When cross-biome WUE_x reaches a
346 maximum that cannot be sustained with further reduction in water availability, minimum WUE_n
347 will also reach a maximum, where WUE_n will approach WUE_x. A non-linear ANPP/ET relation
348 (not shown) will follow as WUE_x and WUE_n approach zero for the most water-limited, low-
349 productivity sites. The inset illustrates the decrease in WUE_x with PDSI for subsets of the

350 LTER₇₅₋₉₈ (n=4), USDA₀₀₋₀₉ (n=5) and Australia₀₁₋₀₉ (n=2) datasets limited to grassland sites,
351 where columns labeled with the same letter are not significantly different ($P > 0.05^{25}$).

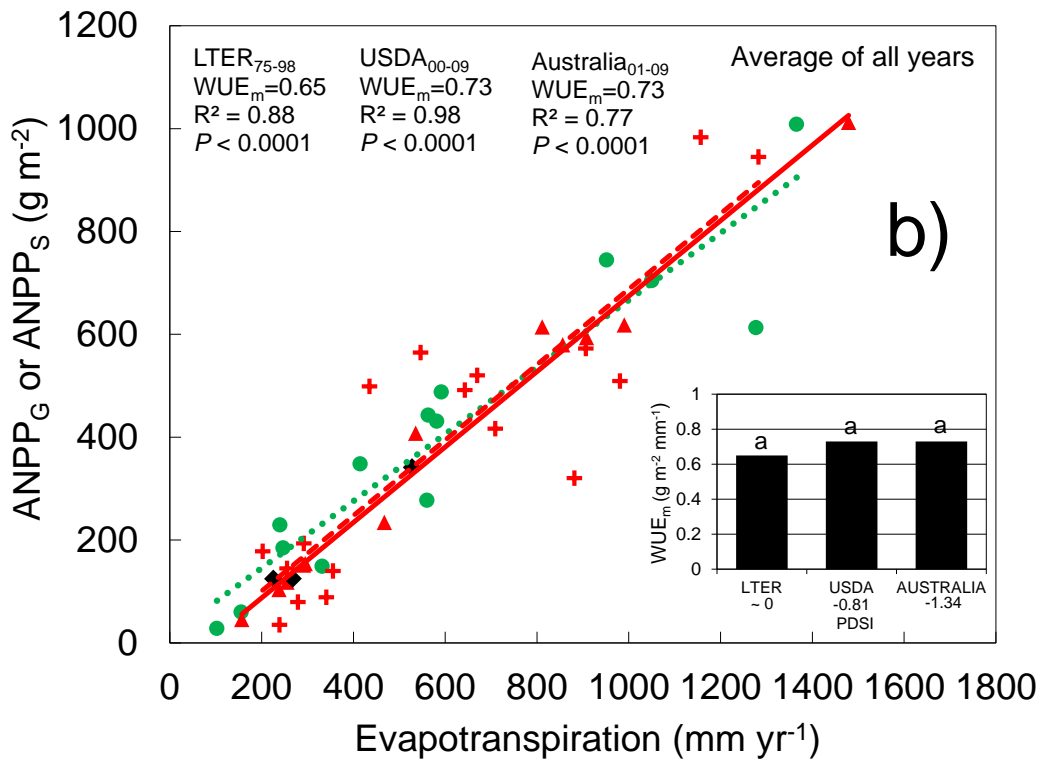
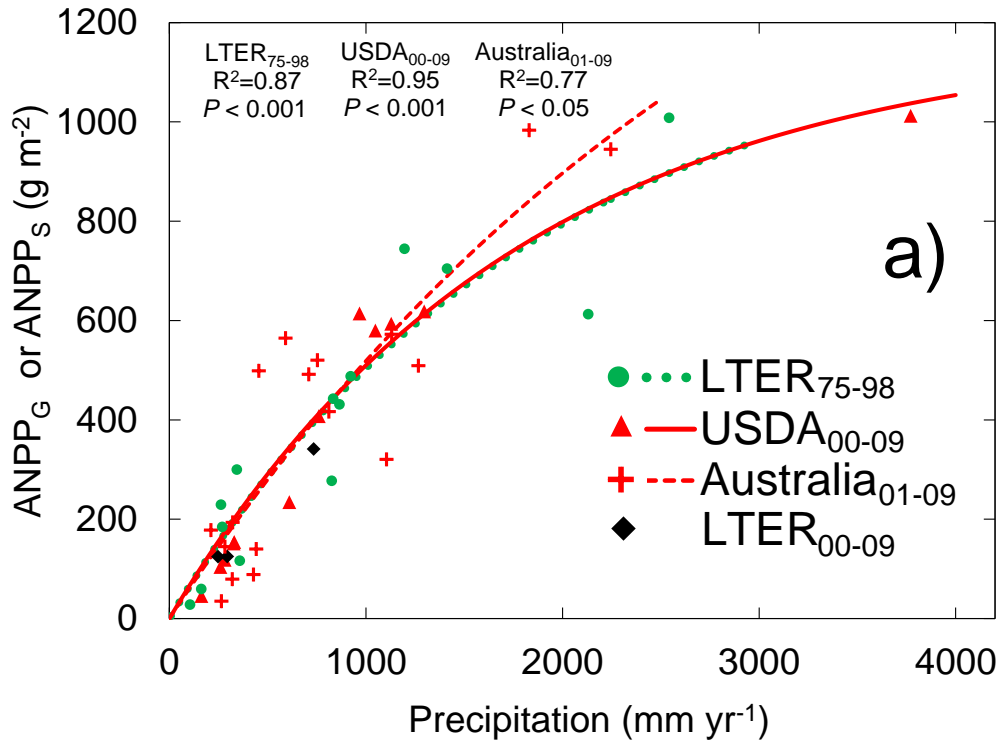
352



353

354 **Figure 1.**

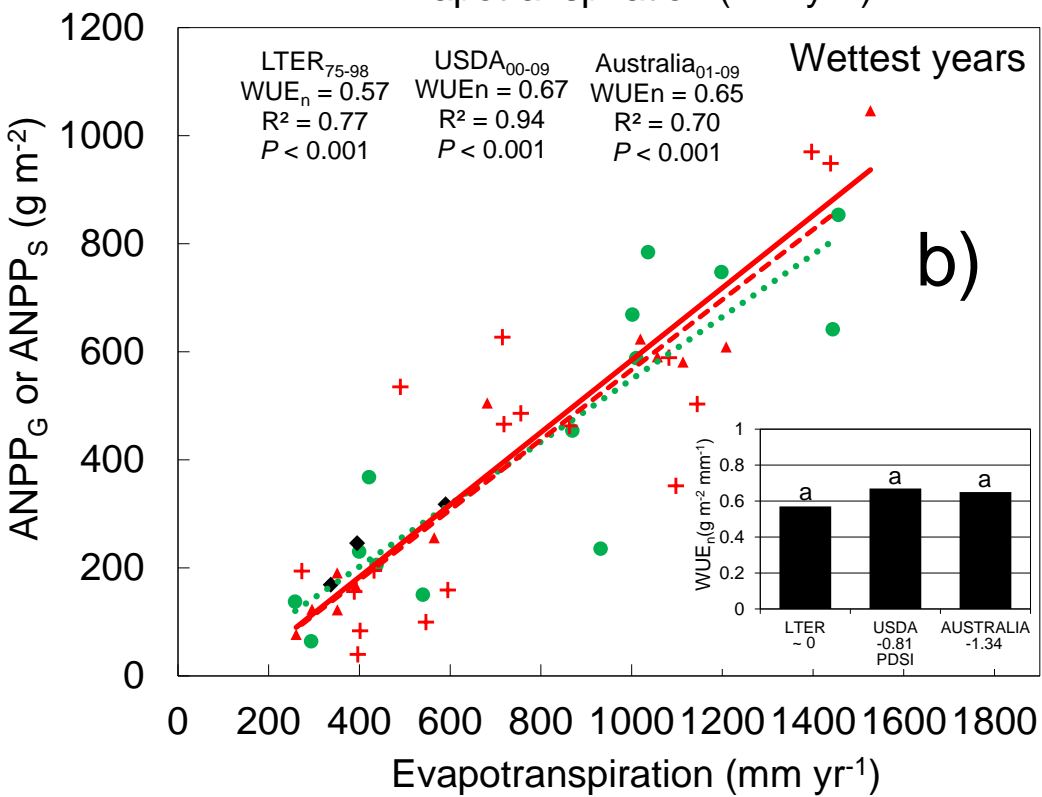
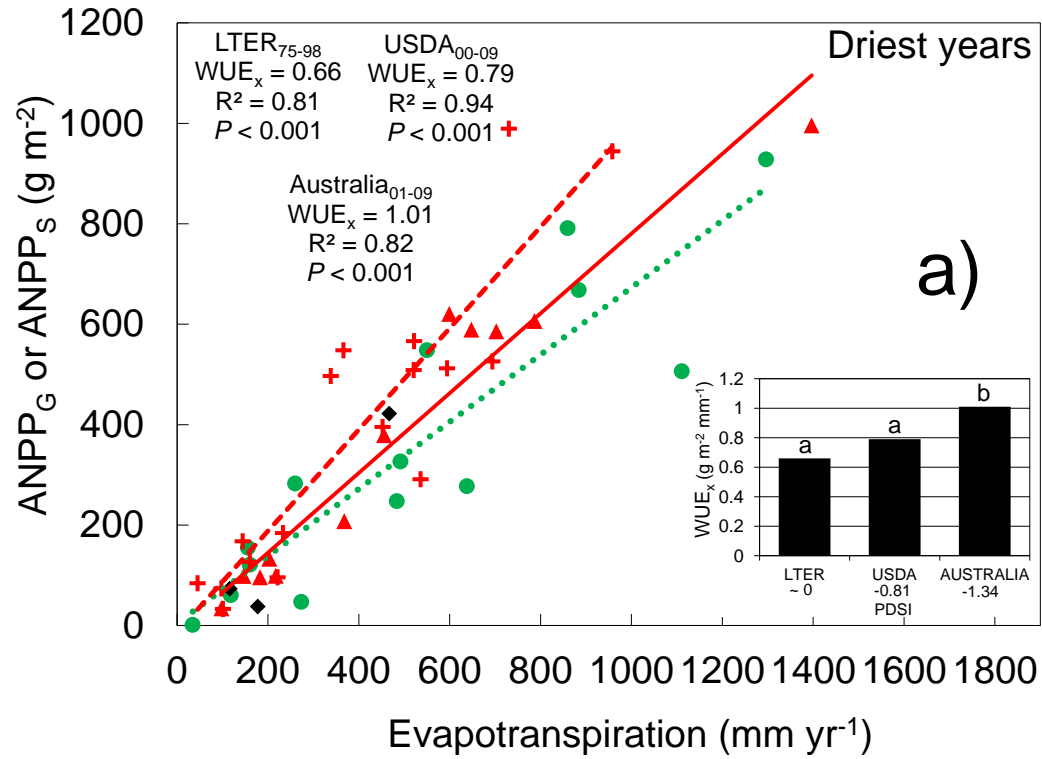
355



356

357 **Figure 2.**

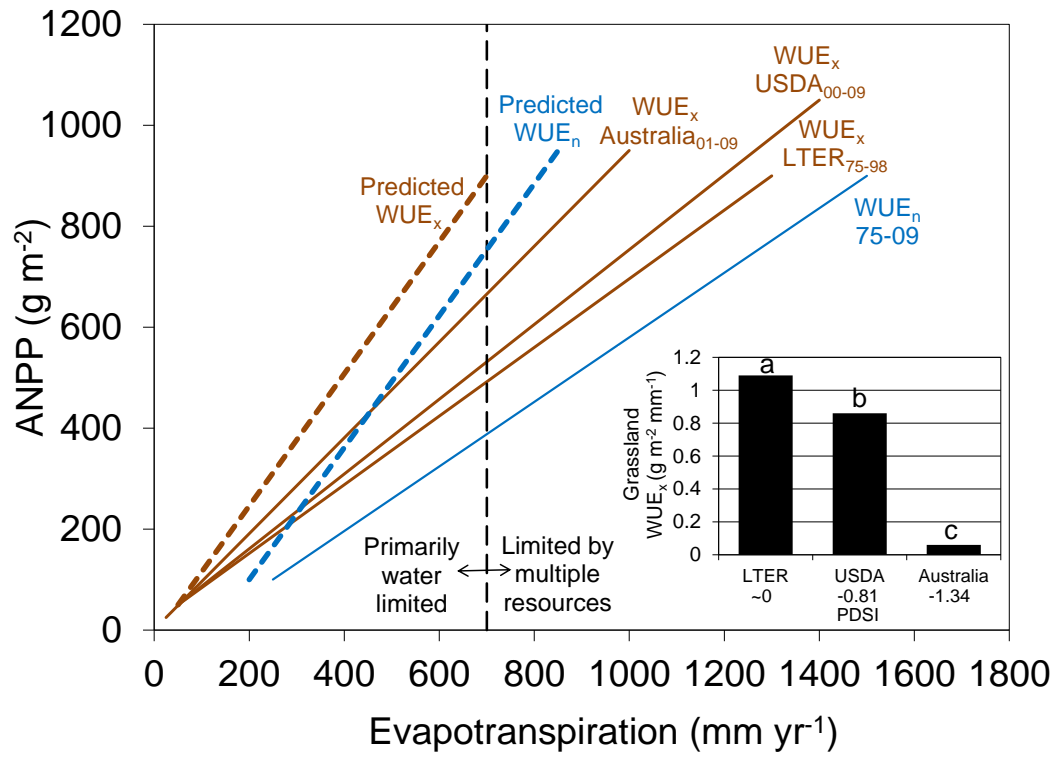
358



359

360 **Figure 3.**

361



362

363 **Figure 4.**